Current Optics and Photonics Vol. 4, No. 3, June 2020, pp. 161-173
ISSN: 2508-7266(Print) / ISSN: 2508-7274(Online) DOI: https://doi.org/10.3807/COPP.2020.4.3.161

Invited Paper

Recent Progress in High-Luminance Quantum Dot Light-Emitting Diodes

Seunghyun Rhee[1], Kyunghwan Kim[1], Jeongkyun Roh[2]*, and Jeonghun Kwak[1]**

[1]*Department of Electrical and Computer Engineering, Inter-university Semiconductor Research Center (ISRC), Seoul National University, Seoul 08826, Korea*
[2]*Department of Electrical Engineering, Pusan National University, Busan 46241, Korea*

(Received March 11, 2020 : revised March 26, 2020 : accepted March 26, 2020)

Colloidal quantum dots (QDs) have gained tremendous attention as a key material for highly advanced display technologies. The performance of QD light-emitting diodes (QLEDs) has improved significantly over the past two decades, owing to notable progress in both material development and device engineering. The brightness of QLEDs has improved by more than three orders of magnitude from that of early-stage devices, and has attained a value in the range of traditional inorganic LEDs. The emergence of high-luminance (HL) QLEDs has induced fresh demands to incorporate the unique features of QDs into a wide range of display applications, beyond indoor and mobile displays. Therefore it is necessary to assess the present status and prospects of HL-QLEDs, to expand the application domain of QD-based light sources. As part of this study, we review recent advances in HL-QLEDs. In particular, based on reports of brightness exceeding 10^5 cd/m^2, we have summarized the major approaches toward achieving high brightness in QLEDs, in terms of material development and device engineering. Furthermore, we briefly introduce the recent progress achieved toward QD laser diodes, being the next step in the development of HL-QLEDs. This review provides general guidelines for achieving HL-QLEDs, and reveals the high potential of QDs as a universal material solution that can enable realization of a wide range of display applications.

Keywords : Quantum dots, High luminance, QLED, QD laser diode
OCIS codes : (130.0250) Optoelectronics; (230.3670) Light-emitting diodes; (160.4236) Nanomaterials

I. INTRODUCTION

Colloidal quantum dots (QDs), which are semiconductor nanoparticles, have attracted considerable attention because of their advantageous features, such as tunable emission spectra (from ultraviolet to infrared), remarkable photoluminescence (PL), and narrow full-width at half-maximum emission bandwidth [1-8]. QDs have been regarded as a key material that can enable next-generation displays, given their advantages of high PL quantum yields (QYs) and cost-effective, solution-based processability [9-15]. Recently, a QD-based color-enhancement film was commercialized successfully in the display market, establishing the superiority of QDs in display applications. Intensive studies are now being conducted to realize the next technology frontier: the replacement of present-day emissive display technologies with QD light-emitting diodes (QLEDs).

The first QD-based electroluminescent device was demonstrated by Colvin *et al.* in 1994 [16]. The luminescence properties of QLEDs improved dramatically over the subsequent two decades with the development of high quality QDs, establishment of the standard *p-i-n* multilayered QLED structure [1, 2, 17-20], improved charge-injection and transport characteristics [2, 20-25], and increased light-extraction efficiency [26-28]. As a result of intensive studies, the luminescence efficiency of QLEDs has improved considerably (by over three orders of magnitude, from 0.01% to >20%) to approach the theoretical maximum [5, 19, 29-32]. Simultaneously, the brightness of QLEDs has increased significantly from the initially demonstrated value

*Corresponding author: jkroh@pusan.ac.kr, ORCID 0000-0002-0674-572X
**Corresponding author: jkwak@snu.ac.kr, ORCID 0000-0002-4037-8687

Color versions of one or more of the figures in this paper are available online.

of 10^2 cd/m^2 to a recently reported value exceeding 10^6 cd/m^2 [33]. As the brightness of QLEDs has improved continuously, to finally equal those in the brightness range of traditional inorganic LEDs (>10^6 cd/m^2), fresh demands to exploit the remarkable features of QLEDs in a wider range of display applications beyond indoor and mobile displays have arisen.

Figure 1(a) shows a broad range of display applications, with respect to required brightness. According to their purposes and operating conditions, displays require different levels of maximum brightness, the so-called *white level*, to guarantee visibility. For example, indoor and mobile displays require a brightness of 10^2~10^3 cd/m^2, whereas public outdoor displays require a higher brightness (>10^3 cd/m^2). When the displays are used in harsh environments such as direct sunlight, brightness exceeding 10^4 cd/m^2 is required to ensure high visibility. Furthermore, when an optical projection-type display is used to provide spatial visualization or magnification, a significantly higher brightness (>10^5 cd/m^2) is necessary to overcome the low transmittance of optical projection systems, which may be less than 1%. In this domain, LEDs with high luminance can be used in low-power projection systems (*e.g.* AR/VR displays). However, a laser diode is a better option for high-power applications such as head-up or cinema displays.

In principle, QDs are expected to be a universal material solution that can cover the entire range of applications with regard to brightness, shown in Fig. 1(a). In the early stages of development, QLEDs were able to cover the low-brightness application regime; at present, they are capable of expanding their applicability to the higher-brightness regime. QD-based light sources covering the brightness regime >10^5 cd/m^2 are termed *high-luminance QLEDs* (HL-QLEDs), to distinguish them from the QLEDs for traditional applications. Furthermore, the remaining region can be covered by developing the final type of QD-based light source: QD laser diodes. This growing adoption of QD-based light sources will provide fresh opportunities to traditional display applications by delivering the unique features of QDs, such as flexibility [14, 28, 34], inexpensive solution processability [13, 31, 35], and conveniently tunable emission color [1-3].

Here, as an aid to boost this growth, we review the recent progress and remaining challenges of HL-QLEDs. We briefly introduce the fundamental operating principles of QLEDs, and then highlight the key factors for achieving HL-QLEDs in terms of two important aspects: material development and device engineering. We summarize the current status of HL-QLEDs with a few important milestones. This is followed by a description of remaining challenges. A review of the key factors impelling HL-QLED technology will guide us to the recent development toward a QD laser diode, which is a longstanding goal in this research field. We cover the most recent research advances in the development of QD laser diodes, and briefly discuss the future prospects. This review introduces the great potential of QDs as a universal material solution to enable a wide range of display applications, and to aid in expanding the application domain of QD-based light sources.

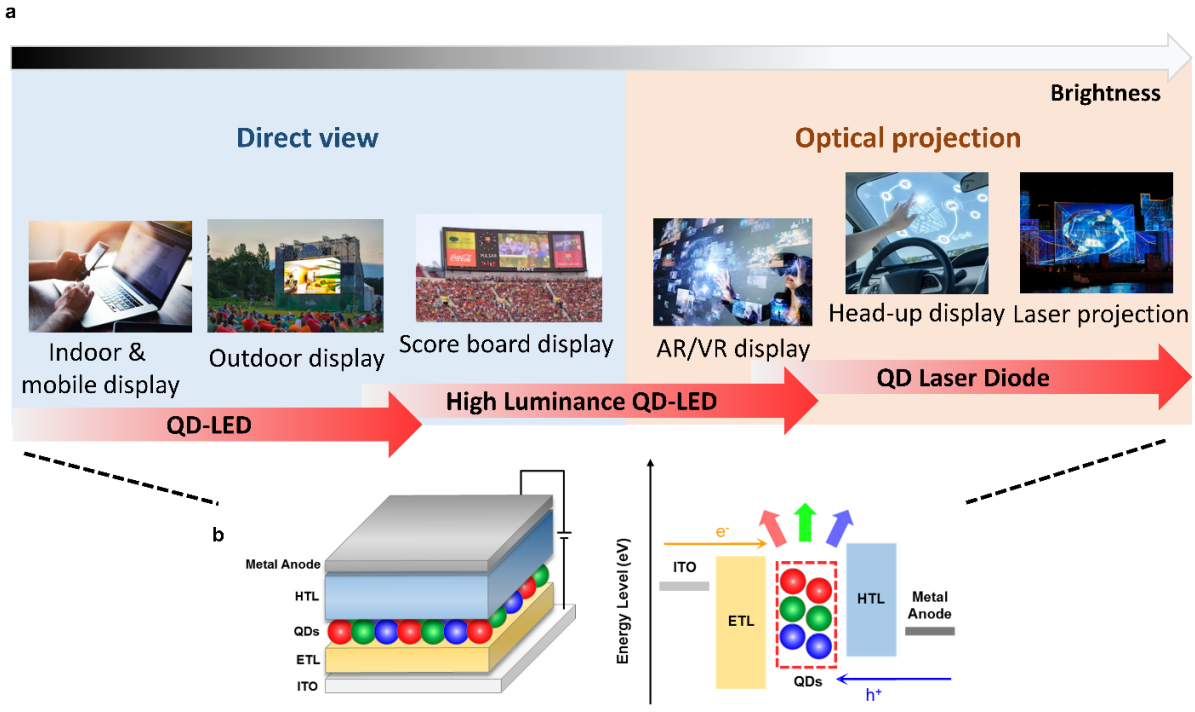

FIG. 1. (a) Display applications of QD-based light sources, with respect to required brightness. (b) Schematic of a standard QLED structure, and its energy-band diagram.

II. METHODS FOR EMPLOYING HL-QLEDS

Intensive studies to improve the performance of QLEDs have resulted in the establishment of a standard device structure based on *p-i-n* multilayers [4, 5, 7, 8, 28, 33, 36]. This state-of-the-art QLED structure comprises a metal anode, hole-transport layer (HTL), QD emissive layer, electron-transport layer (ETL), and an ITO cathode, as shown in Fig. 1(b). The HTL and ETL transfer charge carriers from each electrode to the QDs. The injected carriers (electrons and holes) recombine within the QDs, which generate photons having energy corresponding to that of the QD band gap. Therefore, as can be derived from the operating principle of QLEDs, HL-QLEDs can be realized by (i) injecting and transporting charges efficiently, (ii) using QDs with high luminescence efficiency (that is PL QY), and (iii) improving the light-extraction property. An additional important factor is the carrier-rich environment of HL-QLEDs due to high-current excitation, which produces multiexciton species in QDs [9, 33, 34]. Therefore, the suppression of multiexciton-related nonradiative recombination, known as Auger recombination, is significant for achieving HL-QLEDs. Intensive studies have been performed to address those key issues. As a result, the brightness of QLEDs has improved continuously and entered the domain of HL-QLEDs (>10^5 cd/m^2), as displayed in Fig. 2 and summarized in Table 1. Since the first demonstration of HL-QLEDs by Kwak *et al.* [2], several studies have reported [4, 5, 7, 8] such high brightness (>10^5 cd/m^2), and Sun *et al.* [33] first reported HL-QLEDs with brightness >10^6 cd/m^2.

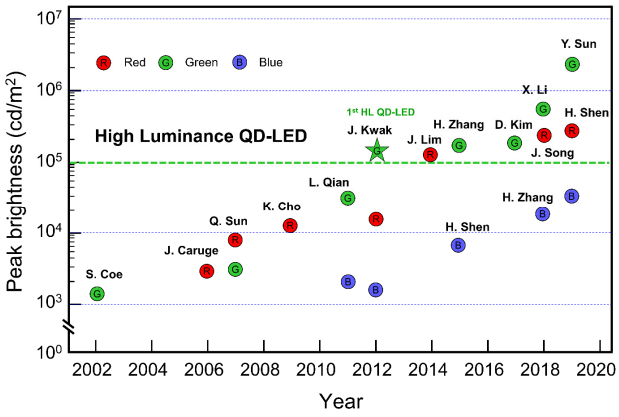

FIG. 2. Development of peak brightness of red, green, and blue QLEDs over time. Data are extracted from references [2, 5, 7, 8, 17, 23, 33, 36-43].

In this chapter, we review key advancements in HL-QLEDs with respect to two aspects: material development and device engineering. First, we overview material-based approaches for achieving HL-QLEDs, which mainly focus on improving the luminescence efficiency of QDs. Then, we cover device-related approaches for HL-QLEDs, which includes engineering of charge-injection properties to improve charge balance, management of heat dissipation, improvement of light extraction, and use of a tandem structure.

2.1. HL-QLEDs Based on Material Modification

A colloidal QD consists of three components: core, shell, and ligands. It is essential to select appropriate materials for each component to achieve highly luminescent QDs. Numerous attempts have been made to improve the luminescence efficiency of QDs, and the following have been identified as the key factors for achieving high luminescence efficiency: (i) selection of an appropriate core/shell structure, and (ii) use of suitable ligands for stable chemical bonding with high conductivity. With regard to the core/shell structure, construction of the shell using a material with a larger band gap than that of the core enhances the luminescence efficiency of QDs noticeably. Therefore, it has become a typical structure for QDs and is called the type-I configuration. Various core/shell material combinations, such as CdSe/ZnS, CdSe/CdS, InP/ZnS, CdSe/ZnSe, and PbS/CdS, have been investigated [44-46].

Type-I core/shell QDs confine electrons and holes in the core efficiently, and consequently improve QLED performance. However, the large difference between the lattice parameters of core and shell in type-I QDs results in

TABLE 1. Summary of QLEDs with peak brightness of over 100,000 cd/m^2

QD type	Peak brightness (cd/m^2)	Emission color	Methods	Ref.
(Cd,Zn)(Se,S)/ZnS	1,680,000	Green	Heat dissipation	33
CdSe/ZnSe	356,000 614,000	Red Green	QD modification	5
CdSe-ZnS-ZnS	460,000	Green	Ligand modification	8
Zn1−xCd$_x$Se/ZnSe/ZnS	334,000	Red	QD modification	7
CdSe/Cd$_x$Zn$_{1-x}$Se/ZnSe$_y$S$_{1-y}$	319,003	Red	QD modification	4
Cd$_x$Zn$_{1-x}$Se/ZnS Cd$_x$Zn$_{1-x}$Se$_y$S$_{1-y}$/ZnS	237,100 576,211	Red Green	Interface engineering	31
(Cd,Zn)(Se,S)/ZnS	115,500	Green	Tandem	36
CdSe/ZnS/ZnS	110,205	Green	Interface engineering	23

inhomogeneous growth of the shell, which produces internal defects in the QDs [45]. These defects are the main obstacles to achieving high luminescence efficiency (QY), because they function as nonradiative recombination centers. The QY is defined by the ratio of radiative recombination rate to the overall recombination rate: $QY = k_r / (k_r + k_{nr})$, where k_r is the rate of radiative recombination and k_{nr} is the rate of nonradiative recombination. It is important to suppress lattice-mismatch-mediated trap states to obtain high QY. Alloyed intermediate-shell and gradient core/shell structures have been proposed to overcome this lattice mismatch and achieve HL-QLEDs.

To reduce the lattice-mismatch-induced traps inside QDs, an intermediate shell is incorporated between core and outer shell. For example, Talapin *et al*. [47] proposed CdSe/CdS/ZnS and CdSe/ZnSe/ZnS core/shell/shell structures for a stepwise variation in lattice parameter from the core to the outer shell. Subsequently, based on this concept, multilayered shell structures (CdSe/CdS/ZnS/CdS-ZnS and CdSe/ZnS/CdS-ZnS) [48] and alloyed multilayered shell structures (CdSe/CdS/$Zn_{0.5}Cd_{0.5}S$/ZnS) [49] have been proposed for stable and high crystallinity of QDs. Bae *et al*. [50] inserted a $CdSe_xS_{1-x}$ alloyed intermediate at a CdSe/CdS core/shell interface; this tactic reduced nonradiative Auger recombination substantially and increased the PL QY of the QDs. Song *et al.* [7] designed a $Zn_{1-x}Cd_xSe$/ZnSe/ZnS alloyed multishell QD structure with an alloyed $Zn_{1-x}Cd_xSe$ core, ZnSe as the middle shell, and ultrathin ZnS as the outer shell; it achieved high PL QY (over 95%) (Fig. 3(a)). Based on the nearly equal valence-band-maximum energies of CdSe and ZnSe, the alloyed $Zn_{1-x}Cd_xSe$ core and ZnSe middle shell display a marginal valence-band (VB) offset and remarkable lattice fringes without defects. QLEDs fabricated with these QDs exhibited outstanding performance (30.9% of peak EQE and 334,000 cd/m^2 peak brightness).

Another highly effective approach that can reduce defects caused by lattice mismatch in QDs is the use of a composition-gradient core/shell structure [4, 6, 35, 51-54]. The gradual change in composition from the core to the shell results in a significantly smoothed lattice-parameter discrepancy, which yields a large reduction of interfacial defects and nonradiative recombination. For example, Dey *et al*. [53] and Zhang *et al*. [54] proposed a gradient-alloyed $CdSe_xS_{1-x}$ QD structure with a CdSe-rich core ($CdSe_{0.8}S_{0.2}$), CdS-rich outer shell ($CdSe_{0.1}S_{0.9}$), and gradual increase in S from core to shell. Similarly, Bae *et al*. [35] and Yang *et al*. [6] recommended an intermediate layer made of gradient-alloyed $Cd_{1-x}Zn_xSe_{1-y}S_y$ between a CdSe-rich core and ZnS-rich outer shell. To minimize the disparity in VB offset with respect to HTL, Shen *et al.* [5] proposed a CdSe/ZnSe core/shell structure. The use of Se throughout the core and shell regions enhances chemical affinity during

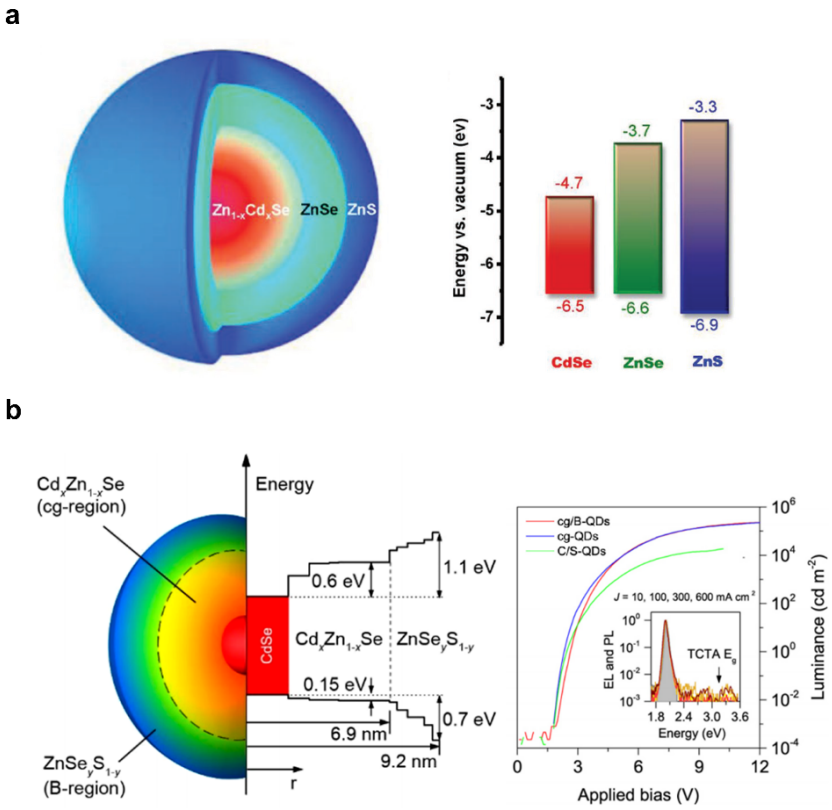

FIG. 3. HL-QLEDs based on material modification. (a) Schematic illustration of $Zn_{1-x}Cd_xSe$/ZnSe/ZnS alloyed multilayered QD structure (left) and energy-level diagram (right). Adapted with permission from [7]. (b) Schematic illustration of continuously graded cg/B-QDs (left) and normalized PL (gray shading) and EL spectra (lines) (right). Adapted with permission from [4].

atomistic growth, resulting in better interfacial properties and a reduction in interfacial defects. The QLED based on this type of QD exhibited high PL QY (>90% for red and green, and 73% for blue) and remarkable device efficiency, with maximum brightness of 356,000 cd/m^2, 614,000 cd/m^2, and 62.600 cd/m^2 for red, green, and blue respectively (the brightness of these red and blue emissions being the highest reported for QLEDs). The gradually varying chemical composition (or energy) of QDs more or less relieves the interfacial strain of the core/shell structure, and improves the PL QY of QDs and performance of QLEDs. In addition, Lim *et al.* [4] synthesized a CdSe/$Cd_xZn_{1-x}Se$/$ZnSe_yS_{1-y}$ structure with a continuously graded (cg) $Cd_xZn_{1-x}Se$ inner shell and a wide-gap $ZnSe_yS_{1-y}$ barrier (B) layer. The inner shell modifies the electron injection into the CdSe core efficiently and enables development of an electron-confinement structure, which can suppress Auger recombination. Meanwhile, the outer barrier of the $ZnSe_yS_{1-y}$ layer (varied by *y*) controls the valance-band and conduction-band (CB) edges of the QD. These eventually equalize the charge injection rate from the CTL to the QD. Devices based on cg/B-QDs exhibited high peak EQE (13.5%) and peak brightness (319,003 cd/m^2), and simultaneously accomplished almost droop-free QLEDs (efficiency reduction of ~3% at 100,000 cd/m^2) (see Fig. 3(b)).

In addition to the core/shell structure, the selection of an appropriate surface ligand is important for achieving high-QY QDs [55, 56]. Ligands play a significant role in both the processability and conductivity of QDs. For example, a long-hydrocarbon-chain ligand (*e.g.* oleic acid or oleylamine) can straightforwardly prevent QD aggregation in organic solvents, but the increased interdot distance can worsen the charge-transport properties of the QD film. Therefore, it is important to exchange long, insulating hydrocarbon-chain ligands for short, conducting ligands, without compromising on QY. To achieve high-QY QDs, the ligand must have (i) a short chain length, to reduce the insulation between the CTLs and QD layers, and (ii) the property of binding strongly to the QD surface, without developing defect states.

Inorganic halogen ions are employed as efficient short ligands to replace long-hydrocarbon ligands, to improve the carrier transport among QDs, and between QDs and adjacent layers. The halide anions I^-, Br^-, and Cl^- have been used to

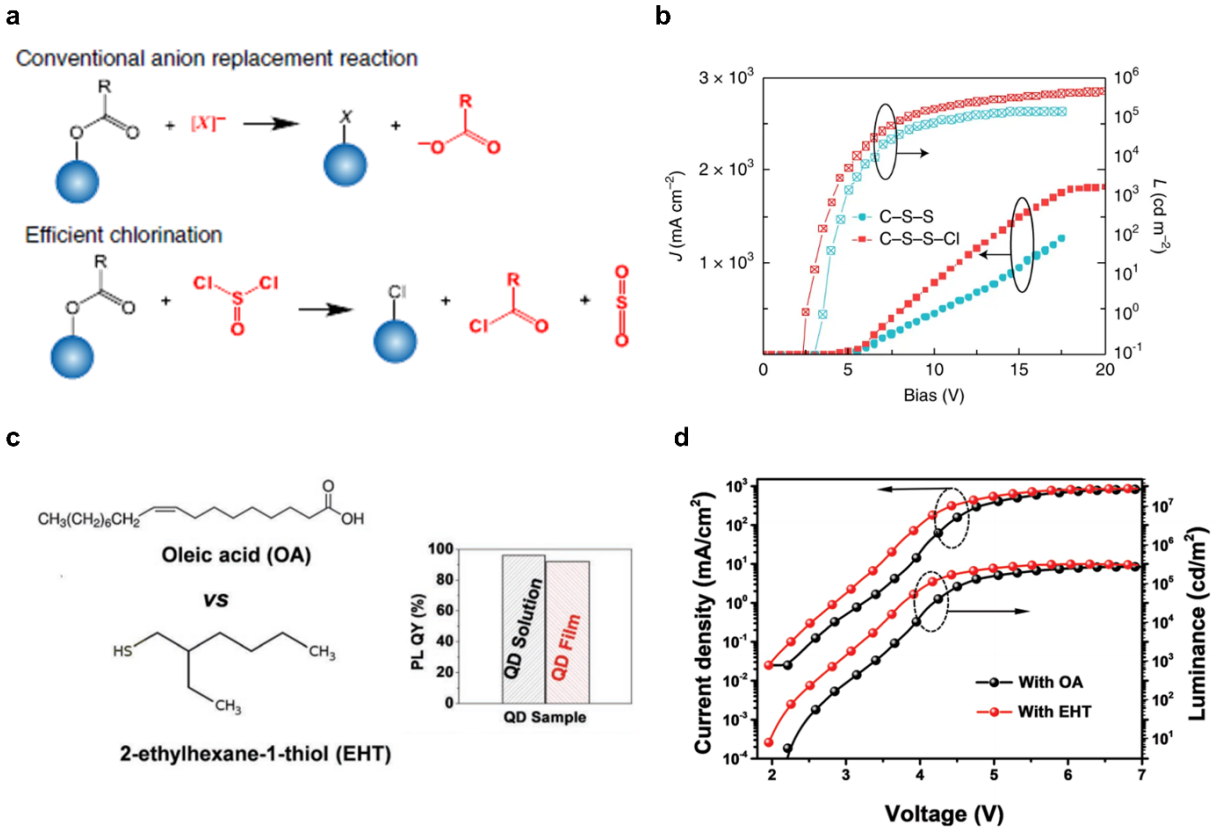

FIG. 4. (a) Chemical equation for efficient chlorination ligand-exchange process. *X* represents pseudohalides, sulfides, metal complexes, etc. The blue spheres and *R* denote CQD and aliphatic hydrocarbon groups respectively. (b) Current-density-luminance-voltage characteristics of the CdSe/ZnS/ZnS core/shell/shell (C/S/S) and C/S/S QDs with chlorination (C/S/S-Cl) -based QLEDs. Adapted with permission from [8]. (c) Chemical structures of oleic acid (OA) and 2-ethylhexane-1-thiol (EHT), and PL QYs of EHT-QDs in solution and solid film. (d) Current-density-luminance-voltage characteristics of QLEDs with OA or EHT surface ligands. Adapted with permission from [7].

stabilize colloidal materials, control interdot distance, and enhance the charge transport of QDs [57, 58]. Kang *et al.* adopted a bromide (Br^-) ligand using cetyltrimethylammonium bromide (CTAB) treatment [58]. This short, conductive ligand enhanced QD-film conductivity. Moreover, the Br-QD-based LED exhibited increased brightness, without decreased PL QY. Li *et al.* proposed an efficient chlorination process that can effectively exchange long-hydrocarbon OA ligands with conductive chloride (Cl^-) ligands using a chlorination reagent ($SOCl_2$), as shown in Fig. 4(a) [8]. This inorganic single-atomic-layer surface ligand reduced the interdot distance of QD films without compromising the PL QY (63% and 60±2% for pristine QD film and Cl-QD film respectively), and enhanced the charge-carrier transport in Cl-QD-based devices. Efficient electron and hole injection can suppress Auger recombination, particularly in the high-current-density region, to result in a high peak brightness of 460,000 cd/m^2 in Cl-QD-based LEDs (Fig. 4(b)).

Owing to its strong binding property, thiol ligands are also widely used as an effective ligand for high-performance QLEDs. The thiol-type ligand, which has relatively short chains for efficient carrier injection and strong anchoring properties on the QD surface, is an electron-donor group that can reduce the VBs of QDs and hole-injection barriers. Shen *et al.* reported 1-octanethiol (OT) ligands on ZnCdS/ZnS graded core/shell QDs, achieving the first reported blue QLEDs with EQE higher than 10% [42]. Li *et al.* also adopted tris (mercaptomethyl)-nonane (TMMN)-capped QDs, which displayed a PL lifetime (9.3 ns) higher than that of OA-capped QDs, owing to the reduced steric hindrance by the shorter ligand chains [59]. Song *et al.* recommended the 2-ethylhexane-1-thiol (EHT) ligand on $Zn_{1-x}Cd_xSe$/ZnSe/ZnS core/shell QDs, which reduces hole injection barrier (between HTL and QDs) from 1.18 eV to 0.91 eV and preserves the high PL QY of QD films (~90%) (Figs. 4(c) and 4(d)) [7].

2.2. HL-QLEDs Based on Device Engineering

Apart from the high PL QY and conductivity of QD materials, the adoption of appropriate device structure significantly affects the achievement of HL-QLEDs. The device structure, ETL, and HTL together determine the carrier-injection properties, carrier confinement in a QD's emissive layer (EML), and the operational stability of QLEDs. Balancing of the injection rates of electrons and holes into the QD EML, and maintenance of operational stability, are the key factors in achieving HL-QLEDs [25, 33, 60]. A disparity between electron and hole injection rates induces nonradiative Auger recombination, resulting in a reduction of the luminance efficiency of a QLED. In addition, the overflow of majority carriers (electrons) to a counter CTL (HTL) accelerates the degradation of organic HTL materials, which attenuates the operational stability of devices [25, 60]. Therefore, various approaches to improving the charge-injection balance in QLEDs have been adopted, in terms of device engineering.

Charge imbalance in QLEDs arises from the different transport and injection capabilities of electrons and holes. For example, ZnO nanoparticles (NPs), the most widely used material for the ETL in a QLED, exhibit a CB energy level highly similar to that of QDs, resulting in straightforward (and occasionally spontaneous) injection of electrons. In contrast, most of the organic hole-transport materials used for the HTL, such as poly(9,9-dioctylfluorene-co-N-(4-(3-methylpropyl))diphenylamine) (TFB), poly(N,N′-bis (4-butylphenyl)-N,N′-bis(phenyl)-benzidine (poly-TPD), poly(9-vinlycarbazole) (PVK), 4,4′-bis(carbazole-9-yl)biphenyl (CBP), and Tris(4-carbazoyl-9-ylphenyl)amine (TCTA), exhibit a large difference in VB energy level from that of QDs. This disrupts efficient injection of holes. Furthermore, the large difference between the electron mobility of ZnO NPs and hole mobility of organic HTL materials worsens the charge imbalance [61, 62]. Various strategies have been recommended to alleviate this disparity, such as enhancing hole injection by modifying the HTL [21, 23-25] and reducing electron injection by ion doping [4, 63, 64] or by inserting an electron-blocking layer (EBL) [19, 65-67]. However, suppressing electron injection results in increased operational stress in QLEDs, so alternative approaches to enhancing hole injection by modulating HTLs in the QLED architecture have been proposed instead.

Unlike the straightforward electron injection/transport using a ZnO NP ETL, hole injection/transport using organic HTLs encounters several obstacles, owing to the large difference in VB level versus QDs and relatively low hole mobilities. Therefore, an inverted QLED structure, which enables the use of deep-VB organic material for the HTL, was proposed to enhance hole injection and device performance. Kwak *et al.* [2] devised the first inverted QLED structure and the first HL-QLEDs exceeding 10^5 cd/m^2. Subsequently, based on this structure several studies were conducted to alleviate the remaining hole-injection barrier in the inverted QLED structure (Fig. 5(a)). Rhee *et al.* [25] reported the insertion of a thin fullerene (C_{60}) interlayer between the hole-injection layer (HIL, MoO_x) and HTL (CBP) to eliminate the universal hole-injection barrier that is created by the pinning effect of MoO_x (Fig. 5(d)). Meanwhile, Jiang *et al.* [22] enhanced hole injection by introducing a 4,4',4''-tri(N-carbazolyl)-triphenyl-amine (TCTA) / N,N'-bis (naphthalen-1-yl)-N,N'-bis (phenyl)-benzidine (NPB) bilayer HTL structure. This structure can be obtained thanks to the high VB of TCTA and the high hole mobility of NPB. Although most of the polymer HTLs used in the conventional QLED structure exhibit a large VB difference from QDs, various studies have been conducted to overcome the hole-injection barrier. Combination of two HTLs also can be an efficient method: For example, Huang *et al.* [21] used a CBP-doped poly-TPD HTL, which can deepen the VB energy level of poly-TPD. Similarly, Li *et al.* [24] recommended the composition of a TPD/PVK HTL structure, which improves hole mobility with TPD and blocks electron suppression from the QD emissive layer. Upshifting the energy level of the QDs by

interfacial engineering can also enhance carrier injection between them and the HTL. Kim *et al.* [23] recommended the incorporation of a polyethylenimine ethoxylated (PEIE) interlayer between the QD emissive layer and poly-TPD, which function as a physical buffer layer and interfacial dipole layer respectively. The QLEDs incorporating PEIE exhibited enhanced carrier injection and thereby achieved high luminance (110,205 cd/m^2) (Figs. 5(b) and 5(c)).

Although the alleviation of charge-injection imbalance can enhance the operational stability of a device by suppressing excessive electron overflow from the QD EML to the HTL, Joule heating (which occurs because of high current density) is a major factor hindering stable operation and high luminance of devices. Previous studies [68-71] have reported that organic films are susceptible to thermal decomposition. Irreversible thermal degradation of organic HTLs can occur during QLED operation; the organic HTL as well as the QD emissive layer are vulnerable to Joule heating. Zhao *et al.* reported that the differing expansion of core and shell due to the thermal energy in QDs can generate inherent defects, resulting in lattice mismatch and reduced PL QY [72].

Therefore, it is important to use QDs that exhibit high thermal stability, and to reduce the heat generated during the operation of HL-QLEDs. Sun *et al.* effectively suppressed Joule heating by employing a thermally efficient substrate (Figs. 5(e) and 5(f)). In addition, they improved the thermal stability of the QDs by exchanging the oleic acid ligand for 1-dodecanethiol. Device roll-off is reduced substantially over a wide luminance range, thanks to the effective dissipation of Joule heat; thereby they achieved the highest reported luminance for green QLEDs (1,680,000 cd/m^2) [33].

Apart from the single-EML-based charge-to-photon conversion process, other methods adopting novel structures for QLEDs have been studied. Although the inherent PL QY of QDs and charge-carrier injection of QLEDs have been developed extensively, only a limited fraction of the total generated photons can be extracted to the exterior of a device [73]. The limited extraction efficiency η_{ext} originates from Snell's law, which states that only a portion of photons can pass through a material with a different refractive index. Therefore, reducing outcoupling loss and enhancing η_{ext} are intuitive methods for improving the brightness of QLEDs [74]. One of the optical structures for increasing η_{ext} is the top-emitting structure, which emits light through its top electrode. This can prevent the large outcoupling loss caused by the substrate [75, 76]. In addition, a remarkable advantage is that the light reflected from the two electrodes can be used to control the cavity effect to improve the color purity and normal-direction brightness of the QLED. Liu *et al.* [26] fabricated top-emitting QLEDs (TQLEDs) with controlled cavity length for enhanced outcoupling efficiency (Fig. 6(a)). TQLEDs exhibiting luminance (112,000 cd/m^2) and current efficiency (27.8 cd/A) significantly higher than those of bottom-emitting devices (9,000 cd/m^2, 13.2 cd/A, respectively) could be achieved by manipulating the thickness of the top Ag electrode and capping layer.

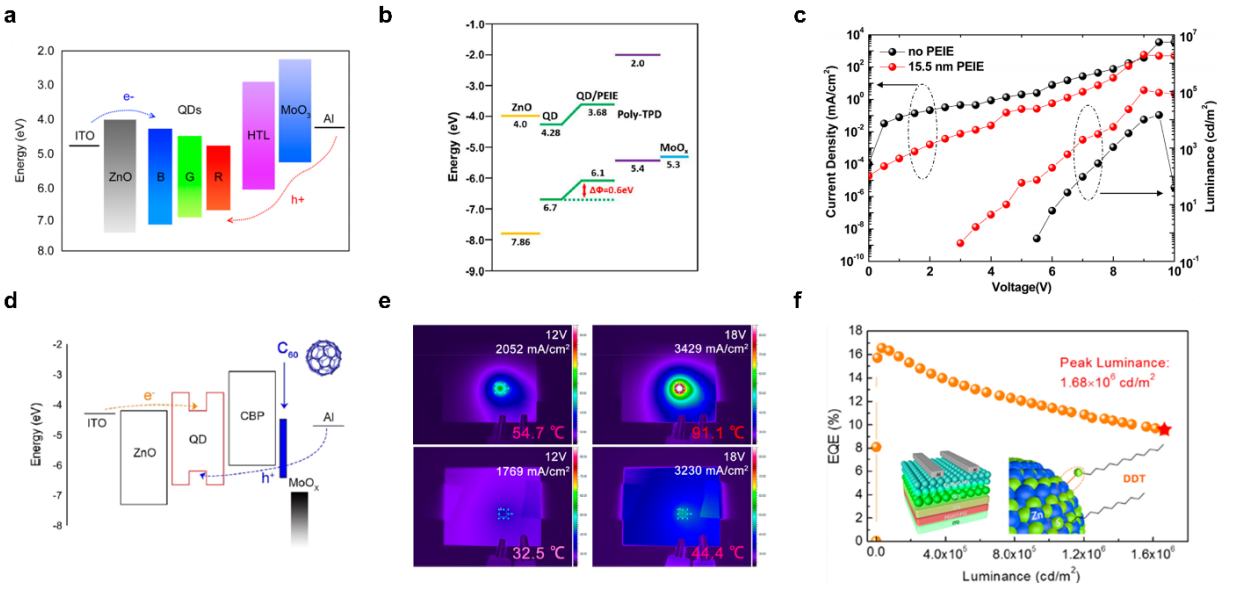

FIG. 5. HL-QLEDs based on device engineering. (a) Energy-band diagram of an inverted QLED structure, for enhanced electron and hole injection. Adapted with permission from [2]. (b) Energy-band diagram of a multilayered QLED showing the upshift of QD VB energy level by a PEIE interlayer. (c) Current-density–luminance–voltage characteristics of QLEDs, with and without a PEIE interlayer. Adapted with permission from [23]. (d) Energy-band diagram of a QLED employing a C_{60} interlayer. Adapted with permission from [25]. (e) Pixel-temperature measurement of operating QLEDs with glass (up) and sapphire (down) substrate, for efficient heat dissipation. (f) EQE–current-density characteristics of sapphire-substrate-based QLEDs (inset: device architecture and anchoring DDT ligand). Adapted with permission from [33].

Outcoupling loss also occurs due to the large difference in the refractive indices of the glass substrate ($n_{glass} \sim 1.5$) and air ($n_{air} = 1$), or metal electrode ($n_{metal} > 1.8$) and air. Therefore, modification of the substrate is required to enhance light extraction to the air. Oh *et al.* [27] effectively prevented total internal reflection at the substrate/air interface by attaching an additional microstructured arrayed film on the substrate of the QLED (Fig. 6(b)). QLEDs featuring an attached microprism or microlens displayed maximum brightnesses that were respectively 1.24 and 1.57 times as high as that of a conventional device.

Meanwhile, increased luminance can be obtained from a double- or triple-EML QLED structure: a tandem structure. A tandem structure adopts two or more electroluminescent (EL) units in a single device, to increase the efficiency and brightness of the QLED. As the multiple EL units are operated at equal current density, the number of photons generated increases proportionally to that the number of of EL units. Zhang *et al.* [36] adopted a tandem structure for QLEDs using (Zn,Mg)O/AL/HAT-CN/MoO_3 as the charge-generation layer. It exhibited high transparency, efficient charge-generation characteristics, and high durability for consecutive solution process (Fig. 6(c)). This tandem QLED displayed high current efficiencies of 17.9, 121.5, and 41.5 cd/A and high brightnesses of 26,800, 115,500, and 65,900 cd/m^2 for blue, green, and red wavelengths respectively.

III. QUANTUM-DOT-BASED LASER DIODES

The significant improvement in QD technologies, in terms of materials and devices, has generated a fresh opportunity to achieve a longstanding goal in this field: the development of a QD-based laser diode. This is the missing piece among QD-based light sources, which would enlarge the application area of projection-type displays by enabling distinguishing features of QDs such as conveniently tunable emission color, flexibility, low weight, and inexpensive processability.

The development of QD laser diodes has been hindered by the intrinsic nature of QDs, wherein light amplification occurs only under multiexciton conditions because of multifold degeneracy of the band-edge states, and excitons decay rapidly by nonradiative Auger recombination [77, 78]. This results in an ultrashort lifetime of optical gain, and complicates lasing in QDs. However, because of the notable progress in material engineering, state-of-the-art QDs exhibit substantially suppressed Auger recombination, which has opened up potential approaches to achieving QD laser diodes [4, 79]. In this chapter, we briefly review the current status of and future prospects for QD laser diodes, with the most recent research advancements.

3.1. Recent Progress Toward QD-based Laser Diodes

A fundamental problem plaguing the development of QD laser diodes is the multiexciton nature of their optical gain [77, 78]. When multiexciton species exist in QDs, rapid nonradiative Auger recombination dominates over radiative recombination, thereby deactivating optical gain [80]. This impedes the realization of lasing in QDs, which requires successive light amplification by spontaneous emission. Furthermore, achievement of lasing in QDs becomes even more challenging when slow electrical excitation is used as a pumping source. Therefore, the development of QDs with suppressed Auger recombination is a prerequisite for the development of QD laser diodes.

Because of the tremendous progress in material engineering (reviewed in Chapter 2), state-of-the art QDs exhibit substantially suppressed Auger decay. As a result, notable progress toward QD laser diodes has been achieved recently. One of the most important milestones was attained by Lim *et al.* [79] using Auger-suppressed cg-QDs to demonstrate population inversion under electrical excitation. Population inversion is a precondition for a laser, in which more electrons are in an excited state than in the ground state, which enables light amplification by stimulated emission. Lim *et al.* constructed QLEDs with a tapered

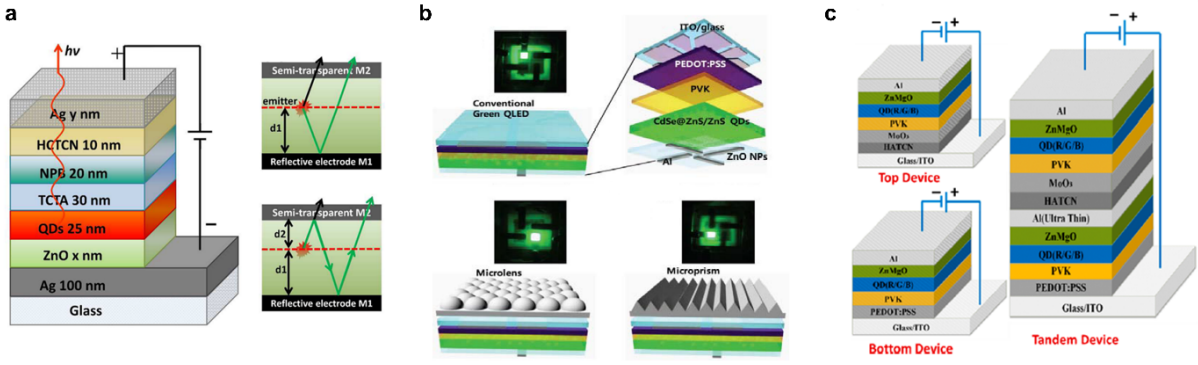

FIG. 6. HL-QLEDs adopting novel structures. (a) Device structure (left) and schematics of the optical model for top-emitting QLEDs (right). Adapted with permission from [26]. (b) Conventional device structure (above) and microlens/microprism-attached light-extracting QLED structure (below). Adapted with permission from [27]. (c) Illustration of QLEDs with top, bottom, and tandem structures. Adapted with permission from [36].

HTL, as shown in Fig. 7(a), to electrically excite cg-QDs with high current densities. Under high-current-density excitation ($J > 1$ A/cm^2), they observed an evident shoulder peak in the EL emission spectrum that was not present at lower current densities (Fig. 7(b)). The emergence of EL emission away from the band-edge emission peak is evidence of the population inversion of the band-edge state, because emission from the higher state becomes feasible only when the lower-energy state is filled completely. They verified this further by measuring the optical gain directly (Fig. 7(c)).

The demonstration of optical gain under electrical excitation resulted in the next step toward QD laser diodes: integration of an optical cavity that can provide an optical-feedback path in an LED structure. Various types of optical cavities, such as Fabry-Perot, whispering-gallery-mode, and distributed-feedback (DFB), can be considered. Roh *et al.* recently reported the first attempt to integrate an optical cavity into a QLED structure [81]. They demonstrated a dual-functioning device that can serve as both an optically pumped laser and an electrically operable LED, as an intermediate step for achieving a laser diode. They fabricated a DFB optical cavity in the bottom indium tin oxide (ITO) electrode, and constructed a standard *p-i-n*-based LED-like device (Fig. 7(d)). By engineering the refractive index of ITO and mode confinement within the QD gain medium, they succeeded in observing strong lasing emission from the LED-like multilayered device under optical excitation, even with an exceptionally thin (50 nm) gain medium, which corresponds to ~3 monolayers of QDs (Fig. 7(e)). This thin gain medium is a favorable feature for electrical excitation. Thereby, they demonstrated that their device is also electrically operable as an LED, with a decent EQE of 4.3% (Fig. 7(f)). However, they did not observe any indication of lasing under electrical excitation, because of current densities insufficient for achieving population inversion. Nonetheless, they stated that their dual-functioning QLED with an integrated optical cavity is a suitable platform for achieving a QD laser diode.

3.2. Future Prospects for QD-based Laser Diodes

Two significant obstacles to achieving QD laser diodes (population inversion under electrical pumping, and integration of optical cavity into the LED structure) have been addressed. The remaining challenge is, in principle, to combine those two efforts: achieving population inversion in a QLED integrated with an optical cavity, under electrical excitation. To increase current densities to a level sufficient for achieving population inversion, short-pulsed operation can be employed to prevent massive heat generation inside the device, or a high-thermal-conductivity substrate can be used for heat management. This should be accompanied by efforts to reduce the lasing threshold, to accommodate this development. The recent demonstration of sub-single-exciton lasing in charged QDs is a good example of a feasible method for reducing the lasing threshold [82].

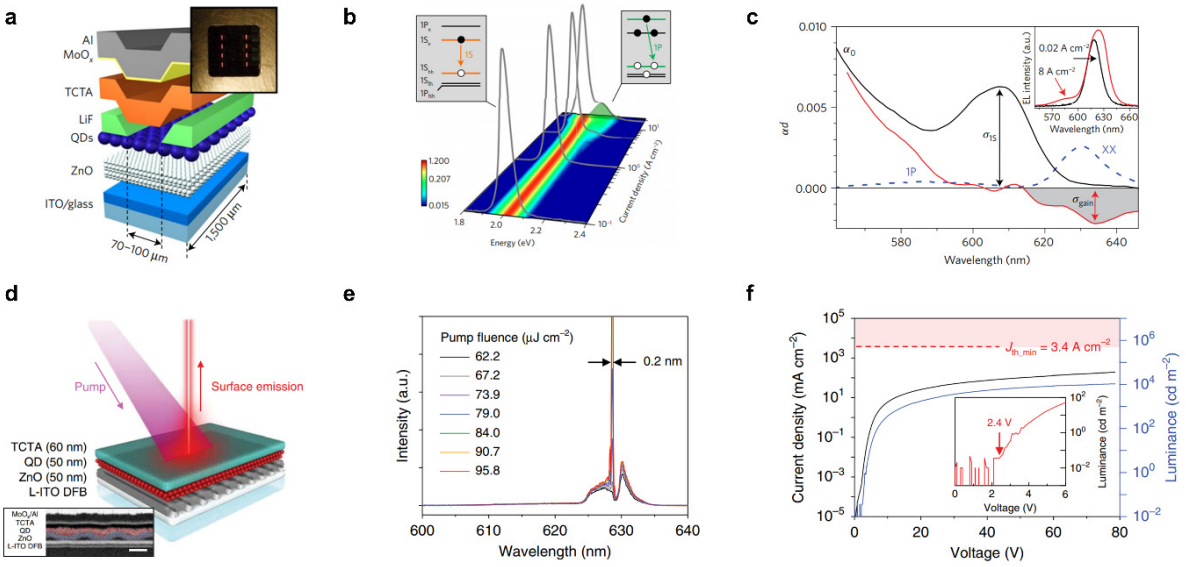

FIG. 7. Quantum-dot-based laser diodes. (a) QLED architecture for boosting the current density to 18 A/cm^2. (b) EL spectra as a function of current density. At high current density (>1 A/cm^2), the EL spectrum shows both 1*S* and 1*P* bands, indicating population inversion under electrical excitation. (c) Optical-gain measurement under electrical pumping, calculated by subtracting the normalized high- and low-current-density EL spectra. Adapted with permission from [79]. (d) Schematic illustration of an optically pumped LED-like structure with a DFB optical cavity. (e) Surface-emission spectrum as a function of pump fluence, showing single-mode lasing at 629 nm. (f) Current-density-voltage-luminance characteristics of QLEDs with an integrated DFB optical cavity. The red dashed line indicates the minimum current density required to achieve population inversion. Adapted with permission from [81].

IV. SUMMARY

This paper has reviewed recent studies aimed at overcoming the obstacles to achieving HL-QLEDs. The status of the development of QD laser diodes was also examined briefly. Various efforts to achieve HL-QLEDs, in terms of material development and device engineering, have been summarized. With regard to material development, the construction of an appropriate QD core/shell structure that can minimize lattice-mismatch-induced traps has been the major focus of research. The use of alloyed or gradient shell structures was observed to be the most efficient method for developing highly luminescent QDs. In addition, the selection of appropriate surface ligands also plays a significant role in realizing high luminance in QDs. Short ligands are preferred, so as not to distort charge transport and injection. Strong chemical bonding with QDs is also important for producing high-quality film with few surface traps. In terms of device engineering, designing a device architecture that can suppress nonradiative Auger recombination by improving charge balance has been the most important research direction for achieving HL-QLEDs. In addition, the moderation of Joule heating, improvement in light-extraction efficiency, and use of tandem structures have also exhibited their effectiveness in improving the luminance of QLEDs.

Notwithstanding this notable progress, several issues remain to be addressed. The first of these is the degraded luminescence efficiency of QDs in films. Although QDs in solution exhibited near-unity PL QY, the PL QY of a QD film still displays considerable suppression, owing to the inherent defects formed during fabrication, and nonradiative Auger recombination by dot interaction. Another issue is the development (or identification) of a better HTL material with a higher hole mobility, closer VB to that of QDs, and most importantly high thermal stability. Present HTL technologies rely substantially on organic materials, but diverse types of materials should be employed and investigated. By solving those remaining challenges, the domain of application for QD-based light sources will be widened, offering fresh opportunities for a wide range of display applications.

ACKNOWLEDGMENT

This study was supported by the Technology Innovation Program (or Industrial Strategic Technology Development Program) (No.10077471) funded by the Ministry of Trade, Industry & Energy (MOTIE, Korea), and the National Research Foundation of Korea (NRF) grant funded by the Korea government (Ministry of Science and ICT) (No. 2020R1C1C1013079).

REFERENCES

1. W. K. Bae, J. Lim, D. Lee, M. Park, H. Lee, J. Kwak, K. Char, C. Lee, and S. Lee, "R/G/B/natural white light thin colloidal quantum dot-based light-emitting devices," Adv. Mater. **26**, 6387-6393 (2014).
2. J. Kwak, W. K. Bae, D. Lee, I. Park, J. Lim, M. Park, H. Cho, H. Woo, D. Y. Yoon, K. Char, S. Lee, and C. Lee, "Bright and efficient full-color colloidal quantum dot light-emitting diodes using an inverted device structure," Nano Lett. **12**, 2362-2366 (2012).
3. S. J. Lim, M. U. Zahid, P. Le, L. Ma, D. Entenberg, A. S. Harney, J. Condeelis, and A. M. Smith, "Brightness-equalized quantum dots," Nat. Commun. **6**, 8210 (2015).
4. J. Lim, Y. S. Park, K. Wu, H. J. Yun, and V. I. Klimov, "Droop-free colloidal quantum dot light-emitting diodes," Nano Lett. **18**, 6645-6653 (2018).
5. H. Shen, Q. Gao, Y. Zhang, Y. Lin, Q. Lin, Z. Li, L. Chen, Z. Zeng, X. Li, Y. Jia, S. Wang, Z. L. Du, L. S. Li, and Z. Zhang, "Visible quantum dot light-emitting diodes with simultaneous high brightness and efficiency," Nat. Photonics **13**, 192-197 (2019).
6. Y. Yang, Y. Zheng, W. Cao, A. Titov, J. Hyvonen, J. R. Manders, J. Xue, P. H. Holloway, and L. Qian, "High-efficiency light-emitting devices based on quantum dots with tailored nanostructures," Nat. Photonics **9**, 259-266 (2015).
7. J. Song, O. Wang, H. Shen, Q. Lin, Z. Li, L. Wang, X. Zhang, and L. S. Li, "Over 30% external quantum efficiency light-emitting diodes by engineering quantum dot-assisted energy level match for hole transport layer," Adv. Funct. Mater. **29**, 1808377 (2019).
8. X. Li, Y.-B. Zhao, F. Fan, L. Levina, M. Liu, R. Quintero-Bermudez, X. Gong, L. N. Quan, J. Fan, Z. Yang, S. Hoogland, O. Voznyy, Z.-H. Lu, and E. H. Sargent, "Bright colloidal quantum dot light-emitting diodes enabled by efficient chlorination," Nat. Photonics **12**, 159-164 (2018).
9. W. K. Bae, Y. S. Park, J. Lim, D. Lee, L. A. Padilha, H. McDaniel, I. Robel, C. Lee, J. M. Pietryga, and V. I. Klimov, "Controlling the influence of Auger recombination on the performance of quantum-dot light-emitting diodes," Nat. Commun. **4**, 2661 (2013).
10. J. M. Pietryga, Y.-S. Park, J. Lim, A. F. Fidler, W. K. Bae, S. Brovelli, and V. I. Klimov, "Spectroscopic and device aspects of nanocrystal quantum dots," Chem. Rev. **116**, 10513-10622 (2016).
11. W. K. Bae and J. Lim, "Nanostructured colloidal quantum dots for efficient electroluminescence devices," Korean J. Chem. Eng. **36**, 173-185 (2019).
12. C. Y. Han and H. Yang, "Development of colloidal quantum dots for electrically driven light-emitting devices," J. Korean Ceram. Soc. **54**, 449-469 (2017).
13. Y. Shang and Z. Ning, "Colloidal quantum-dots surface and device structure engineering for high-performance light-emitting diodes," Natl. Sci. Rev. **4**, 170-183 (2017).
14. M. K. Choi, J. Yang, T. Hyeon, and D.-H. Kim, "Flexible quantum dot light-emitting diodes for next-generation displays," npj Flexible Electron. **2**, 10 (2018).
15. F. Chen, Z. Guan, and A. Tang, "Nanostructure and device architecture engineering for high-performance quantum-dot light-emitting diodes," J. Mater. Chem. C **6**, 10958-10981

(2018).
16. V. L. Colvin, M. C. Schlamp, and A. P. Alivisatos, "Light-emitting-diodes made from cadmium selenide nanocrystals and a semiconducting polymer," Nature **370**, 354-357 (1994).
17. S. Coe, W. K. Woo, M. Bawendi, and V. Bulovic, "Electro-luminescence from single monolayers of nanocrystals in molecular organic devices," Nature **420**, 800-803 (2002).
18. A. H. Mueller, M. A. Petruska, M. Achermann, D. J. Werder, E. A. Akhadov, D. D. Koleske, M. A. Hoffbauer, and V. I. Klimov, "Multicolor light-emitting diodes based on semiconductor nanocrystals encapsulated in GaN charge injection layers," Nano Lett. **5**, 1039-1044 (2005).
19. X. Dai, Z. Zhang, Y. Jin, Y. Niu, H. Cao, X. Liang, L. Chen, J. Wang, and X. Peng, "Solution-processed, high-performance light-emitting diodes based on quantum dots," Nature **515**, 96-99 (2014).
20. J. Lim, S. Jun, E. Jang, H. Baik, H. Kim, and J. Cho, "Preparation of highly luminescent nanocrystals and their application to light-emitting diodes," Adv. Mater. **19**, 1927-1932 (2007).
21. Q. Huang, J. Pan, Y. Zhang, J. Chen, Z. Tao, C. He, K. Zhou, Y. Tu, and W. Lei, "High-performance quantum dot light-emitting diodes with hybrid hole transport layer via doping engineering," Opt. Express **24**, 25955-25963 (2016).
22. C. Jiang, H. Liu, B. Liu, Z. Zhong, J. Zou, J. Wang, L. Wang, J. Peng, and Y. Cao, "Improved performance of inverted quantum dots light emitting devices by introducing double hole transport layers," Org. Electron. **31**, 82-89 (2016).
23. D. Kim, Y. Fu, S. Kim, W. Lee, K.-H. Lee, H. K. Chung, H.-J. Lee, H. Yang, and H. Chae, "Polyethylenimine ethoxylated-mediated all-solution-processed high-performance flexible inverted quantum dot-light-emitting device," ACS Nano **11**, 1982-1990 (2017).
24. J. Li, Z. Liang, Q. Su, H. Jin, K. Wang, G. Xu, and X. Xu, "Small molecule-modified hole transport layer targeting low turn-on-voltage, bright, and efficient full-color quantum dot light emitting diodes," ACS Appl. Mater. Interfaces **10**, 3865-3873 (2018).
25. S. Rhee, J. H. Chang, D. Hahm, K. Kim, B. G. Jeong, H. J. Lee, J. Lim, K. Char, C. Lee, and W. K. Bae, ""Positive incentive" approach to enhance the operational stability of quantum dot-based light-emitting diodes," ACS Appl. Mater. Interfaces **11**, 40252-40259 (2019).
26. G. Liu, X. Zhou, and S. Chen, "Very bright and efficient microcavity top-emitting quantum dot light-emitting diodes with Ag electrodes," ACS Appl. Mater. Interfaces **8**, 16768-16775 (2016).
27. J. H. Oh, D. B. Choi, K. H. Lee, H. Yang, and Y. R. Do, "Enhanced light extraction from green quantum dot light-emitting diodes by attaching microstructure arrayed films," IEEE J. Sel. Top. Quantum Electron. **22**, 42-47 (2016).
28. K. Ding, Y. Fang, S. Dong, H. Chen, B. Luo, K. Jiang, H. Gu, L. Fan, S. Liu, B. Hu, and L. Wang, "24.1% external quantum efficiency of flexible quantum dot light-emitting diodes by light extraction of silver nanowire transparent electrodes," Adv. Opt. Mater. **6**, 1800347 (2018).
29. B. S. Mashford, M. Stevenson, Z. Popovic, C. Hamilton, Z. Zhou, C. Breen, J. Steckel, V. Bulovic, M. Bawendi, S. Coe-Sullivan, and P. T. Kazlas, "High-efficiency quantum-dot light-emitting devices with enhanced charge injection," Nat. Photonics **7**, 407-412 (2013).
30. L. Wang, J. Lin, Y. Hu, X. Guo, Y. Lv, Z. Tang, J. Zhao, Y. Fan, N. Zhang, Y. Wang, and X. Liu, "Blue quantum dot light-emitting diodes with high electroluminescent efficiency," ACS Appl. Mater. Interfaces **9**, 38755-38760 (2017).
31. Y. Fu, W. Jiang, D. Kim, W. Lee, and H. Chae, "Highly efficient and fully solution-processed inverted light-emitting diodes with charge control interlayers," ACS Appl. Mater. Interfaces **10**, 17295-17300 (2018).
32. Y.-H. Won, O. Cho, T. Kim, D.-Y. Chung, T. Kim, H. Chung, H. Jang, J. Lee, D. Kim, and E. Jang, "Highly efficient and stable InP/ZnSe/ZnS quantum dot light-emitting diodes," Nature **575**, 634-638 (2019).
33. Y. Sun, Q. Su, H. Zhang, F. Wang, S. Zhang, and S. Chen, "Investigation on thermally induced efficiency roll-off: toward efficient and ultrabright quantum-dot light-emitting diodes," ACS Nano **13**, 11433-11442 (2019).
34. Y. Altintas, S. Genc, M. Y. Talpur, and E. Mutlugun, "CdSe/ZnS quantum dot films for high performance flexible lighting and display applications," Nanotechnology **27**, 295604 (2016).
35. W. K. Bae, K. Char, H. Hur, and S. Lee, "Single-step synthesis of quantum dots with chemical composition gradients," Chem. Mat. **20**, 531-539 (2008).
36. H. Zhang, S. Chen, and X. W. Sun, "Efficient red/green/blue tandem quantum-dot light-emitting diodes with external quantum efficiency exceeding 21%," ACS Nano **12**, 697-704 (2018).
37. Q. Sun, Y. A. Wang, L. S. Li, D. Wang, T. Zhu, J. Xu, C. Yang, and Y. Li, "Bright, multicoloured light-emitting diodes based on quantum dots," Nat. Photonics **1**, 717-722 (2007).
38. K.-S. Cho, E. K. Lee, W.-J. Joo, E. Jang, T.-H. Kim, S. J. Lee, S.-J. Kwon, J. Y. Han, B. K. Kim, B. L. Choi, and J. M. Kim, "High-performance crosslinked colloidal quantum-dot light-emitting diodes," Nat. Photonics **3**, 341-345 (2009).
39. L. Qian, Y. Zheng, J. Xue, and P. H. Holloway, "Stable and efficient quantum-dot light-emitting diodes based on solution-processed multilayer structures," Nat. Photonics **5**, 543-548 (2011).
40. J. Lim, B. G. Jeong, M. Park, J. K. Kim, J. M. Pietryga, Y.-S. Park, V. I. Klimov, C. Lee, D. C. Lee, and W. K. Bae, "Influence of shell thickness on the performance of light-emitting devices based on CdSe/$Zn_{1-X}Cd_XS$ core/shell heterostructured quantum dots," Adv. Mater. **26**, 8034-8040 (2014).
41. J.-M. Caruge, J. E. Halpert, V. Bulović, and M. G. Bawendi, "NiO as an inorganic hole-transporting layer in quantum-dot light-emitting devices," Nano Lett. **6**, 2991-2994 (2006).
42. H. Shen, W. Cao, N. T. Shewmon, C. Yang, L. S. Li, and J. Xue, "High-efficiency, low turn-on voltage blue-violet quantum-dot-based light-emitting diodes," Nano Lett. **15**, 1211-1216 (2015).
43. H. Zhang, X. Sun, and S. Chen, "Over 100 cd A^{-1} efficient quantum dot light-emitting diodes with inverted tandem structure," Adv. Funct. Mater. **27**, 1700610 (2017).
44. B. O. Dabbousi, J. Rodriguez-Viejo, F. V. Mikulec, J. R. Heine, H. Mattoussi, R. Ober, K. F. Jensen, and M. G. Bawendi, "(CdSe) ZnS core-shell quantum dots: synthesis and characterization of a size series of highly luminescent

nanocrystallites," J. Phys. Chem. B **101**, 9463-9475 (1997).
45. X. Peng, M. C. Schlamp, A. V. Kadavanich, and A. P. Alivisatos, "Epitaxial growth of highly luminescent CdSe/CdS core/shell nanocrystals with photostability and electronic accessibility," J. Am. Chem. Soc. **119**, 7019-7029 (1997).
46. D. V. Talapin, A. L. Rogach, A. Kornowski, M. Haase, and H. Weller, "Highly luminescent monodisperse CdSe and CdSe/ZnS nanocrystals synthesized in a hexadecylamine-trioctylphosphine oxide-trioctylphospine mixture," Nano Lett. **1**, 207-211 (2001).
47. D. V. Talapin, I. Mekis, S. Götzinger, A. Kornowski, O. Benson, and H. Weller, "CdSe/CdS/ZnS and CdSe/ZnSe/ZnS core-shell-shell nanocrystals," J. Phys. Chem. B **108**, 18826-18831 (2004).
48. E. Jang, S. Jun, H. Jang, J. Llim, B. Kim, and Y. Kim, "White-light-emitting diodes with quantum dot color converters for display backlights," Adv. Mater. **22**, 3076-3080 (2010).
49. R. Xie, U. Kolb, J. Li, T. Basché, and A. Mews, "Synthesis and characterization of highly luminescent CdSe-Core CdS/$Zn_{0.5}Cd_{0.5}S$/ZnS multishell nanocrystals," J. Am. Chem. Soc. **127**, 7480-7488 (2005).
50. W. K. Bae, L. A. Padilha, Y. S. Park, H. McDaniel, I. Robel, J. M. Pietryga, and V. I. Klimov, "Controlled alloying of the core-shell interface in CdSe/CdS quantum dots for suppression of auger recombination," ACS Nano **7**, 3411-3419 (2013).
51. J. Lim, M. Park, W. K. Bae, D. Lee, S. Lee, C. Lee, and K. Char, "Highly efficient cadmium-free quantum dot light-emitting diodes enabled by the direct formation of excitons within InP@ZnSeS quantum dots," ACS Nano **7**, 9019-9026 (2013).
52. R. E. Bailey and S. Nie, "Alloyed semiconductor quantum dots: Tuning the optical properties without changing the particle size," J. Am. Chem. Soc. **125**, 7100-7106 (2003).
53. S. Dey, S. Chen, S. Thota, M. R. Shakil, S. L. Suib, and J. Zhao, "Effect of gradient alloying on photoluminescence blinking of single CdS_xSe_{1-x} nanocrystals," J. Phys. Chem. C **120**, 20547-20554 (2016).
54. J. Zhang, Q. Yang, H. Cao, C. I. Ratcliffe, D. Kingston, Q. Y. Chen, J. Ouyang, X. Wu, D. M. Leek, F. S. Riehle, and K. Yu, "Bright gradient-alloyed $CdSexS_{1-x}$ quantum dots exhibiting cyan-blue emission," Chem. Mater. **28**, 618-625 (2016).
55. D. Kim and D. C. Lee, "Surface ligands as permeation barrier in the growth and assembly of anisotropic semiconductor nanocrystals," J. Phys. Chem. Lett. **11**, 2647-2657 (2020).
56. H. Lee, D.-E. Yoon, S. Koh, M. S. Kang, J. Lim, and D. C. Lee, "Ligands as a universal molecular toolkit in synthesis and assembly of semiconductor nanocrystals," Chem. Sci. **11**, 2318-2329 (2020).
57. H. Zhang, J. Jang, W. Liu, and D. V. Talapin, "Colloidal nanocrystals with inorganic halide, pseudohalide, and halometallate ligands," ACS Nano **8**, 7359-7369 (2014).
58. B.-H. Kang, J.-S. Lee, S.-W. Lee, S.-W. Kim, J.-W. Lee, S.-A. Gopalan, J.-S. Park, D.-H. Kwon, J.-H. Bae, H.-R. Kim, and S.-W. Kang, "Efficient exciton generation in atomic passivated CdSe/ZnS quantum dots light-emitting devices," Sci. Rep. **6**, 34659 (2016).
59. Z. Li, Y. Hu, H. Shen, Q. Lin, L. Wang, H. Wang, W. Zhao, and L. S. Li, "Efficient and long-life green light-emitting diodes comprising tridentate thiol capped quantum dots," Laser Photon. Rev. **11**, 1600227 (2017).
60. J. H. Chang, P. Park, H. Jung, B. G. Jeong, D. Hahm, G. Nagamine, J. Ko, J. Cho, L. A. Padilha, D. C. Lee, C. Lee, K. Char, and W. K. Bae, "Unraveling the origin of operational instability of quantum dot based light-emitting diodes," ACS Nano **12**, 10231-10239 (2018).
61. H. Shen, Q. Lin, W. Cao, C. Yang, N. T. Shewmon, H. Wang, J. Niu, L. S. Li, and J. Xue, "Efficient and long-lifetime full-color light-emitting diodes using high luminescence quantum yield thick-shell quantum dots," Nanoscale **9**, 13583-13591 (2017).
62. X. Xiong, C. Wei, L. Xie, M. Chen, P. Tang, W. Shen, Z. Deng, X. Li, Y. Duan, W. Su, H. Zeng, and Z. Cui, "Realizing 17.0% external quantum efficiency in red quantum dot light-emitting diodes by pursuing the ideal inkjet-printed film and interface," Org. Electron. **73**, 247-254 (2019).
63. Y. Lee, B. G. Jeong, H. Roh, J. Roh, J. Han, D. C. Lee, W. K. Bae, J. Y. Kim, and C. Lee, "Enhanced lifetime and efficiency of red quantum dot light-emitting diodes with Y-doped ZnO sol-gel electron-transport layers by reducing excess electron injection," Adv. Quantum Technol. **1**, 1700006 (2018).
64. J.-H. Kim, C.-Y. Han, K.-H. Lee, K.-S. An, W. Song, J. Kim, M. S. Oh, Y. R. Do, and H. Yang, "Performance improvement of quantum dot-light-emitting diodes enabled by an alloyed ZnMgO nanoparticle electron transport layer," Chem. Mater. **27**, 197-204 (2015).
65. X. Jin, C. Chang, W. Zhao, S. Huang, X. Gu, Q. Zhang, F. Li, Y. Zhang, and Q. Li, "Balancing the electron and hole transfer for efficient quantum dot light-emitting diodes by employing a versatile organic electron-blocking layer," ACS Appl. Mater. Interfaces **10**, 15803-15811 (2018).
66. Z. Li, "Enhanced performance of quantum dots light-emitting diodes: The case of Al_2O_3 electron blocking layer," Vacuum **137**, 38-41 (2017).
67. I. Cho, H. Jung, B. G. Jeong, J. H. Chang, Y. Kim, K. Char, D. C. Lee, C. Lee, J. Cho, and W. K. Bae, "Multifunctional dendrimer ligands for high efficiency, solution-processed quantum dot light-emitting diodes," ACS Nano **11**, 684-692 (2017).
68. J.-R. Gong, L.-J. Wan, S.-B. Lei, C.-L. Bai, X.-H. Zhang, and S.-T. Lee, "Direct evidence of molecular aggregation and degradation mechanism of organic light-emitting diodes under joule heating: an STM and photoluminescence study," J. Phys. Chem. B **109**, 1675-1682 (2005).
69. D. Y. Kondakov, W. C. Lenhart, and W. F. Nichols, "Operational degradation of organic light-emitting diodes: Mechanism and identification of chemical products," J. Appl. Phys. **101**, 024512 (2007).
70. S. Schmidbauer, A. Hohenleutner, and B. König, "Chemical degradation in organic light-emitting devices: mechanisms and implications for the design of new materials," Adv. Mater. **25**, 2114-2129 (2013).
71. K. Yoshida, T. Matsushima, Y. Shiihara, H. Kuwae, J. Mizuno, and C. Adachi, "Joule heat-induced breakdown of organic thin-film devices under pulse operation," J. Appl.

Phys. **121**, 195503 (2017).
72. Y. Zhao, C. Riemersma, F. Pietra, R. Koole, C. D. Donegá, and A. Meijerink, "High-temperature luminescence quenching of colloidal quantum dots," ACS Nano **6**, 9058-9067 (2012).
73. Q. Yue, W. Li, F. Kong, and K. Li, "Enhancing the out-coupling efficiency of organic light-emitting diodes using two-dimensional periodic nanostructures," Adv. Mater. Sci. Eng. **2012**, 985762 (2012).
74. W. D. Kim, D. Kim, D.-E. Yoon, H. Lee, J. Lim, W. K. Bae, and D. C. Lee, "Pushing the efficiency envelope for semiconductor nanocrystal-based electroluminescence devices using anisotropic nanocrystals," Chem. Mater. **31**, 3066-3082 (2019).
75. G. W. Park, S. J. Lee, and J. H. Ko, "Comparison of out-coupling efficiency between bottom-emission and top-emission organic light-emitting diodes using FDTD simulation," J. Nanoelectron. Optoelectron. **11**, 229-233 (2016).
76. S. Hofmann, M. Thomschke, B. Lüssem, and K. Leo, "Top-emitting organic light-emitting diodes," Opt. Express **19**, A1250-A1264 (2011).
77. V. I. Klimov, A. A. Mikhailovsky, S. Xu, A. Malko, J. A. Hollingsworth, C. A. Leatherdale, H. J. Eisler, and M. G. Bawendi, "Optical gain and stimulated emission in nano-crystal quantum dots," Science **290**, 314-317 (2000).
78. F. Fan, O. Voznyy, R. P. Sabatini, K. T. Bicanic, M. M. Adachi, J. R. McBride, K. R. Reid, Y. S. Park, X. Li, A. Jain, R. Quintero-Bermudez, M. Saravanapavanantham, M. Liu, M. Korkusinski, P. Hawrylak, V. I. Klimov, S. J. Rosenthal, S. Hoogland, and E. H. Sargent, "Continuous-wave lasing in colloidal quantum dot solids enabled by facet-selective epitaxy," Nature **544**, 75-79 (2017).
79. J. Lim, Y.-S. Park, and V. I. Klimov, "Optical gain in colloidal quantum dots achieved with direct-current electrical pumping," Nat. Mater. **17**, 42-49 (2018).
80. Y. S. Park, W. K. Bae, T. Baker, J. Lim, and V. I. Klimov, "Effect of auger recombination on lasing in heterostructured quantum dots with engineered core/shell interfaces," Nano Lett. **15**, 7319-7328 (2015).
81. J. Roh, Y.-S. Park, J. Lim, and V. I. Klimov, "Optically pumped colloidal-quantum-dot lasing in LED-like devices with an integrated optical cavity," Nat. Commun. **11**, 271 (2020).
82. O. V. Kozlov, Y.-S. Park, J. Roh, I. Fedin, T. Nakotte, and V. I. Klimov, "Sub-single-exciton lasing using charged quantum dots coupled to a distributed feedback cavity," Science **365**, 672-675 (2019).